MEMORANDUM
RM-3884-PR
DECEMBER 1963

ELECTROMAGNETIC SIGNALS PRODUCED BY LOW-ALTITUDE NUCLEAR EXPLOSIONS

W. J. Karzas and R. Latter

PREPARED FOR:
UNITED STATES AIR FORCE PROJECT RAND

The RAND Corporation
SANTA MONICA • CALIFORNIA

MEMORANDUM

RM-3884-PR

DECEMBER 1963

ELECTROMAGNETIC SIGNALS PRODUCED BY LOW-ALTITUDE NUCLEAR EXPLOSIONS

W. J. Karzas and R. Latter

This research is sponsored by the United States Air Force under Project RAND—contract No. AF 49(638)-700 monitored by the Directorate of Development Planning, Deputy Chief of Staff, Research and Development, Hq USAF. Views or conclusions contained in this Memorandum should not be interpreted as representing the official opinion or policy of the United States Air Force.

The RAND Corporation

1700 MAIN ST • SANTA MONICA • CALIFORNIA

PREFACE AND SUMMARY

The general nature of the electromagnetic signals from nuclear explosions, as they appear at great distances, is reasonably understood. However, near the explosions, in the region ionized by the gamma rays, the electromagnetic phenomena have been less explored experimentally and are less well understood theoretically. The present report bears on the phenomena in this near–in region.

Specifically, a simplified model of the explosion is treated analytically. The model assumes the explosion takes place at a height h above an infinitely conducting ground. The ambient air is assumed to have a uniform and constant conductivity, and the explosion is approximated as a point source of gamma rays.

This model is solved analytically for the magnetic field at any point about the explosion. Some numerical results illustrate the time and space variation of the magnetic field.

ELECTROMAGNETIC SIGNALS PRODUCED BY LOW-ALTITUDE NUCLEAR EXPLOSIONS

We shall treat approximately the electromagnetic radiation from an explosion at height h above an infinitely conducting ground plane. It will be assumed that the radiating current source is a delta function in time which propagates at the speed of light radially through the air. The air is assumed to have a uniform and constant conductivity. In addition, in order to simulate the effect of the most intensely ionized region surrounding the burst point, the radiating current will be assumed to be zero inside a sphere of radius r_c about the burst point (see Figure 1).

Under these assumptions, the $\vec{B}$-field can be shown from Maxwell's equations

$$\nabla \times \vec{B} = \frac{1}{c} \frac{\partial \vec{E}}{\partial t} + \frac{4\pi\sigma}{c} \vec{E} + \frac{4\pi}{c} \vec{j} \tag{1}$$

$$\nabla \times \vec{E} = - \frac{1}{c} \frac{\partial \vec{B}}{\partial t} \tag{2}$$

to satisfy the wave equation

$$\nabla^2 \vec{B} - \frac{1}{c^2} \frac{\partial^2 \vec{B}}{\partial t^2} - \frac{4\pi\sigma}{c^2} \frac{\partial \vec{B}}{\partial t} = - \frac{4\pi}{c} \nabla \times \vec{j} . \tag{3}$$

Equation (3) can be solved for arbitrary $\vec{j}$ and constant σ. To do so, we first take the Fourier transform of Eq. (3) with respect to

$\vec{r}$. Thus

$$\frac{\partial^2 \hat{\vec{B}}}{\partial t^2} + 4\pi\sigma \frac{\partial \hat{\vec{B}}}{\partial t} + c^2 k^2 \hat{\vec{B}} = -4\pi i c \vec{k} \times \hat{\vec{j}}, \tag{4}$$

where

$$\vec{B} = \frac{1}{(2\pi)^3} \int d\vec{k} e^{-i\vec{k}\cdot\vec{r}} \hat{\vec{B}}. \tag{5}$$

Next we take the Laplace transform of Eq. (4) with respect to t, obtaining

$$\hat{\hat{\vec{B}}} = -4\pi i c \frac{\vec{k} \times \hat{\hat{\vec{j}}}}{s^2 + 4\pi\sigma s + c^2 k^2}, \tag{6}$$

where it is assumed that $\vec{j}$ and $\vec{B}$ are zero at $t = 0$ and

$$\hat{\vec{B}} = \frac{1}{2\pi i} \int_{a-i\infty}^{a+i\infty} ds e^{st} \hat{\hat{\vec{B}}}. \tag{7}$$

From Eqs. (5), (6), and (7), we find that

$$\vec{B} = -\frac{c}{4\pi^3} \int d\vec{k} \int_{a-i\infty}^{a+i\infty} ds e^{-i\vec{k}\cdot\vec{r} + st} \frac{\vec{k} \times \hat{\hat{\vec{j}}}}{s^2 + 4\pi\sigma s + c^2 k^2}. \tag{8}$$

Or

$$\vec{B} = \frac{2c}{\pi} \int_0^t d\tau e^{-2\pi\sigma(t-\tau)} \int d\vec{r}' \frac{\nabla_{r'} \times \vec{j}(\vec{r}', \tau)}{|\vec{r} - \vec{r}'|} I(|\vec{r} - \vec{r}'|, t - \tau), \tag{9}$$

where

$$I\left(|\vec{r}-\vec{r}'|,\, t-\tau\right) = -\int_0^\infty dk \sin k|\vec{r}-\vec{r}'| \; \frac{k \sin(t-\tau)\sqrt{c^2k^2-4\pi^2\sigma^2}}{\sqrt{c^2k^2-4\pi^2\sigma^2}} \,. \qquad (10)$$

A relatively straightforward evaluation of Eq. (10) gives

$$I\left(|\vec{r}-\vec{r}'|,\, t-\tau\right) = \frac{\pi}{2c}\,\delta\left(c(t-\tau)-|\vec{r}-\vec{r}'|\right) - \frac{2\pi^2\sigma}{c^3}\,|\vec{r}-\vec{r}'|\,\frac{I_1\left(2\pi\sigma\sqrt{(t-\tau)^2-|\vec{r}-\vec{r}'|^2/c^2}\right)}{\sqrt{(t-\tau)^2-|\vec{r}-\vec{r}'|^2/c^2}} \qquad (11)$$

Substituting Eq. (11) into Eq. (9) yields the final result:

$$\vec{B}(\vec{r},t) = \frac{1}{c}\int d\vec{r}'\,\frac{e^{-2\pi\sigma|\vec{r}-\vec{r}'|/c}}{|\vec{r}-\vec{r}'|}\,\nabla_{r'}\times\vec{j}(\vec{r}',t_{ret}=t-|\vec{r}-\vec{r}'|/c) - \frac{4\pi\sigma}{c^2}\int d\vec{r}'\int_0^{t-|\vec{r}-\vec{r}'|/c} d\tau e^{-2\pi\sigma(t-\tau)}\nabla_{r'}\times\vec{j}(\vec{r}',\tau)\,\frac{I_1\left(2\pi\sigma\sqrt{(t-\tau)^2-|r-r'|^2/c^2}\right)}{\sqrt{(t-\tau)^2-|\vec{r}-\vec{r}'|^2/c^2}} \qquad (12)$$

For the assumed character of the radiating current and for the geometry of Fig. 1, we have

$$\vec{j} = j_o\,\frac{e^{-r/\lambda}}{r^2}\,\delta(t-r/c)\;u\left(\cos\theta+\frac{h}{r}\right)\;u\left(r-r_c\right)\;\vec{e}_r + \vec{j}\,(\text{image}) \qquad (13)$$

where $u(x) = 0 \quad x < 0,$

$= 1 \quad x > 0;$

so that

$$\nabla \times \vec{j} = 2j_o \frac{e^{-r/\lambda}}{r^3} \delta(t-r/c)\sin\theta\,\delta(\cos\theta + \frac{h}{r})\, u\,(r-r_c)\, e_\varphi , \quad (14)$$

where

$$j_o = - \frac{e R_e \eta Y}{4\pi\lambda E_\gamma} .$$

e is the electron charge; R_e, the electron range in air; η, the fraction of the yield, Y, emitted as gamma rays; λ, the gamma-ray mean-free-path in air; and E_γ is the mean energy of the gammas.

Substituting Eq. (14) into Eq. (12), we find by straightforward evaluation (see Appendix I) that the magnetic field at height a above the ground surface is

$$B(\rho,\ z = a, t) = \{B_1(\rho, a, t) + B_2(\rho, a, t)\}\, \vec{e}_\varphi \quad (15)$$

where for

$$ct \geq \sqrt{\rho^2 + (h+a)^2} ,$$

we have

$$B_1(\rho, a, t) = 4\frac{j_o}{\rho} e^{-2\pi\sigma t}(B - A) \int_o^1 ds\, \frac{e^{-(1/\lambda - 2\pi\sigma/c)\chi}}{\chi^2}\, u(\chi - r_c)$$

$$\frac{\rho^2 - h^2 - c^2t^2 + 2ct\chi + a^2}{\sqrt{\left(\rho + \sqrt{\chi^2 - h^2}\right)^2 - (ct-\chi)^2 + a^2}\sqrt{(ct-\chi)^2 - a^2 - \left(\rho - \sqrt{\chi^2 - h^2}\right)^2}} \quad (16)$$

and

$$B_2(\rho, a, t) = -\frac{16\pi\sigma}{c^2}\frac{j_o}{\rho}e^{-2\pi\sigma t}\int_{r_c}^{B} dz\, e^{-(1/\lambda - 2\pi\sigma/c)z}\int_{\sqrt{a^2+(\rho-\sqrt{z^2-h^2})^2}}^{\sqrt{a^2+(\rho+\sqrt{z^2-h^2})^2}} dy\, yu(t-\frac{y+z}{c})$$

$$\cdot \frac{\rho^2 - h^2 + z^2 - y^2 + a^2}{\sqrt{\left(\rho+\sqrt{z^2-h^2}\right)^2 - y^2 + a^2}\sqrt{y^2 - a^2 - \left(\rho-\sqrt{z^2-h^2}\right)^2}} \frac{I_1(2\pi\sigma\sqrt{(t-z/c)^2 - y^2/c^2})}{\sqrt{(t-z/c)^2 - y^2/c^2}}, \tag{17}$$

where

$$\chi = (B - A)\, s + A$$

$$B = \frac{ct(h^2 - \rho^2 - a^2 + (ct)^2) + \rho\sqrt{\left(h^2 + \rho^2 - a^2 - (ct)^2\right)^2 + 4a^2\left(\rho^2 - (ct)^2\right)}}{2\left((ct)^2 - \rho^2\right)},$$

$$A = \frac{ct(h^2 - \rho^2 - a^2 + (ct)^2) - \rho\sqrt{(h^2 + \rho^2 - a^2 - (ct)^2)^2 + 4a^2(\rho^2 - (ct)^2)}}{2\left((ct)^2 - \rho^2\right)},$$

$u(\chi) = 0$ if $\chi < 0$,

$= 1$ if $\chi \geq 0$.

For $ct < \sqrt{\rho^2 + (h+a)^2}$, $B_1 = B_2 = 0$.

In the case that the radiating current has an arbitrary time dependence specified, say, by the function $f(t)$, the magnetic field

can be obtained from Eq. (15) by (see Appendix II)

$$\vec{B}_f(\rho,\ z = a, t) = \int_0^t d\tau\, f(t-\tau)\, \vec{B}(\rho,\ z = a, \tau). \qquad (18)$$

DISCUSSION

The magnetic field of Eqs. (15) to (17) has been evaluated numerically for a set of representative parameter values. In all calculations, a , the height of the observation point, was set equal to zero, which is the case of greatest practical interest. The results are presented in Figs. 2 to 18.

Using these results, the magnetic field may be determined for a particular explosion by specifying the time variation of the gamma-ray emission and carrying out the integration of Eq. (18).

For the early time behavior, this procedure is quite accurate. However, when the air conductivity becomes large (the saturation phase), the procedure becomes poor.

After the saturation phase, the procedure improves again. However, during this latter phase, the gamma-ray source—mainly the delayed fission gammas and the neutron-capture (in air) gammas—is somewhat extended in space. It is therefore necessary to carry out an additional spacial integration of Eq. (18) to account for the extended source behavior of the gamma-ray emission.

APPENDIX I

We shall derive here Eqs. (15) – (17) from Eqs. (12) – (14). To obtain $B_1(\rho, t)$ we substitute Eq. (14) into the first term of Eq. (12) and make use of the geometry of Fig. 1. Then

$$B_1(\rho, a, t) = \frac{2j_o}{c} \int r'^2 dr' \int d\varphi' \cos\varphi' \int d\theta' \sin^2\theta' \frac{e^{-2\pi\sigma R/c}}{R}$$

$$\cdot \frac{e^{-r'/\lambda}}{r'^3} \delta\left(t - \frac{r' + R}{c}\right) \delta\left(\cos\theta' + \frac{h}{r'}\right) \qquad \text{(I. 1)}$$

Carrying out the θ'–integration, changing variables from (r', φ) to $(\chi = r', R)$, and then integrating over R, we obtain

$$B_1(\rho, a, t) = \frac{4j_o}{\rho} e^{-2\pi\sigma t} \int_A^B d\chi \frac{e^{-(1/\lambda - 2\pi\sigma/c)\chi}}{\chi^2} u(\chi - r_c)$$

$$\cdot \frac{\rho^2 + \chi^2 - h^2 - (ct - \chi)^2 + a^2}{\sqrt{\left(\rho + \sqrt{\chi^2 - h^2}\right)^2 - (ct - \chi)^2 + a^2} \sqrt{(ct - \chi)^2 - a^2 - \left(\rho - \sqrt{\chi^2 - h^2}\right)^2}} \cdot$$

(I. 2)

Letting

$$\chi = (B - A)\, s + A \,,$$

Eq. (I. 2) reduces to Eq. (16).

To obtain $B_2(\rho, t)$, we proceed similarly to $B_1(\rho, t)$ and substitute Eq. (14) into the second term of Eq. (12). Using the geometry of Fig. 1, we find

$$B_2(\rho, a, t) = -\frac{8\pi\sigma}{c^2} j_o \int r'^2 dr' \int d\varphi' \cos\varphi' \int d\theta' \sin^2\theta' \int_o^{t-R/c} d\tau e^{-2\pi\sigma(t-\tau)} \cdot \frac{e^{-r'/\lambda}}{r'^3} \delta(\tau - r'/c)\, \delta\left(\cos\theta' + \frac{h}{r'}\right) \frac{I_1\left(2\pi\sigma\sqrt{(t-\tau)^2 - R^2/c^2}\right)}{\sqrt{(t-\tau)^2 - R^2/c^2}} . \tag{I.3}$$

As before—carrying out the θ'-integration, changing variables from (r', φ', τ) to (r', R, τ), and integrating over τ, we obtain

$$B_2(\rho, a, t) = -\frac{12\pi\sigma}{c^2} \frac{j_o}{\rho} \int_{r_c}^{B} dr' \int_{\sqrt{a^2 + (\rho - \sqrt{r'^2 - h^2})^2}}^{\sqrt{a^2 + (\rho + \sqrt{r'^2 - h^2})^2}} R\, dR \, \frac{e^{-r'/\lambda}}{r'^2} \cdot \frac{\rho^2 + r'^2 - h^2 - R^2 + a^2}{\sqrt{(\rho + \sqrt{r'^2 - h^2})^2 - R^2 + a^2}\, \sqrt{R^3 - a^2 - (\rho - \sqrt{r'^2 - h^2})^2}}$$

$$u\left(t - \frac{r' + R}{c}\right) e^{-2\pi\sigma(t - r'/c)} \frac{I_1\left(2\pi\sigma\sqrt{(t - r'/c)^2 - R^2/c^2}\right)}{\sqrt{(t - r'/c)^2 - R^2/c^2}} ,$$

which is identical with Eq. (17).

APPENDIX II

It should be noted that $B(\rho, z, \tau)$ has a strong singular dependence on the "cut-off" radius r_c arising from the $B_1(\rho, z, t)$ term. In particular, for $0 < r_c << \rho$, a straightforward evaluation of Eq. (16) for $h = a = 0$ and for small $ct - \rho$ shows that

$$B_1 \approx - \frac{4\pi\sqrt{2}\, j_o}{\rho^{3/2}\sqrt{ct-\rho}}\, e^{-2\pi\sigma t}\left[\int_o^{\rho/2\lambda} dx\, e^{-x} I_o(x) - \frac{1}{\pi}\sqrt{\frac{\rho}{r_c}}\,\sqrt{1-\frac{ct-\rho}{2r_c}}\right] ,$$

$$\text{for } ct-\rho < 2r_c ,$$

$$\approx - \frac{4\pi\sqrt{2}\, j_o}{\rho^{3/2}\sqrt{ct-\rho}}\, e^{-2\pi\sigma t} \int_o^{\rho/2\lambda} dx\, e^{-x} I_o(x),$$

$$\text{for } ct-\rho > 2r_c .$$

The importance of the term in r_c is that it leads to a change in polarity of B_1 at early times and moreover its integral over time is independent of r_c, namely,

$$\frac{4\sqrt{2}\, j_o}{\rho^{3/2}}\sqrt{\frac{\rho}{r_c}} \int_{\rho/c}^{\rho/c+2r_c/c} dt\, \frac{1}{\sqrt{ct-\rho}}\sqrt{1-\frac{ct-\rho}{2r_c}} = \frac{4\pi j_o}{\rho c} ,$$

which behavior is analogous to that of a δ - function.

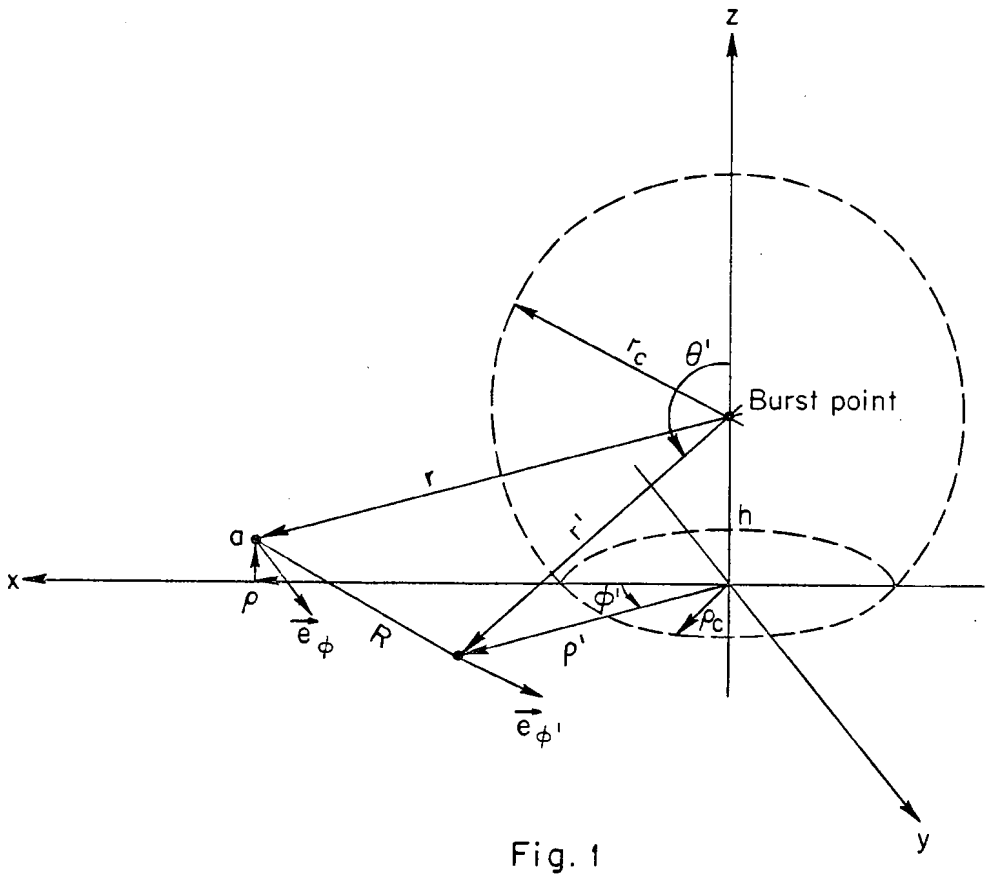
z
r_c
θ'
Burst point
r
h
a
r'
x
ρ
$\vec{e}_\phi$
R
ϕ'
ρ_c
ρ'
$\vec{e}_{\phi'}$
y

Fig. 1

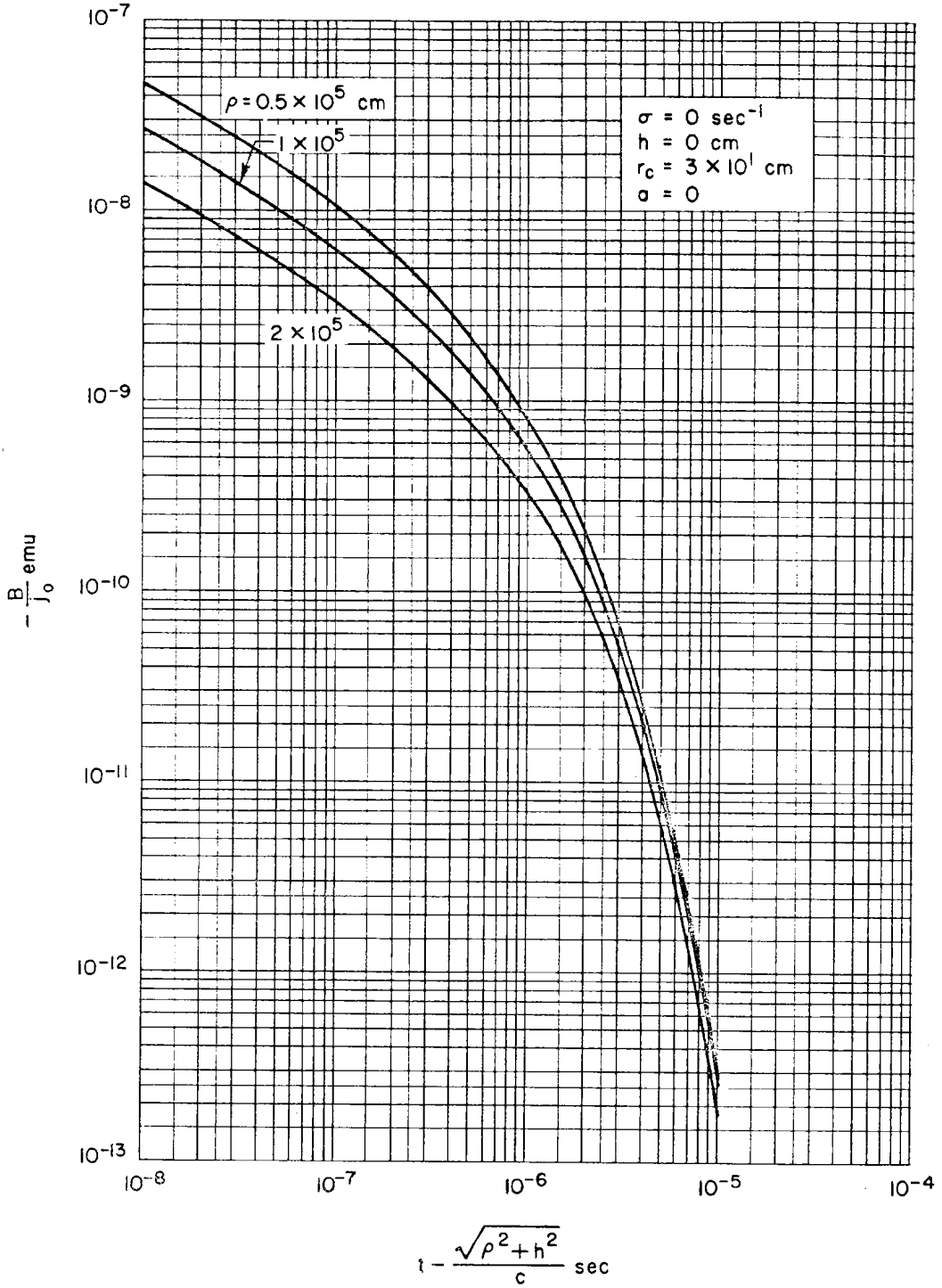
10^{-7}
10^{-8}
10^{-9}
10^{-10}
10^{-11}
10^{-12}
10^{-13}
$-\frac{B}{J_o}$ emu
$\rho = 0.5 \times 10^5$ cm
1×10^5
2×10^5
$\sigma = 0$ sec^{-1}
$h = 0$ cm
$r_c = 3 \times 10^1$ cm
$a = 0$
10^{-8}
10^{-7}
10^{-6}
10^{-5}
10^{-4}
$t - \frac{\sqrt{\rho^2+h^2}}{c}$ sec

Fig. 2

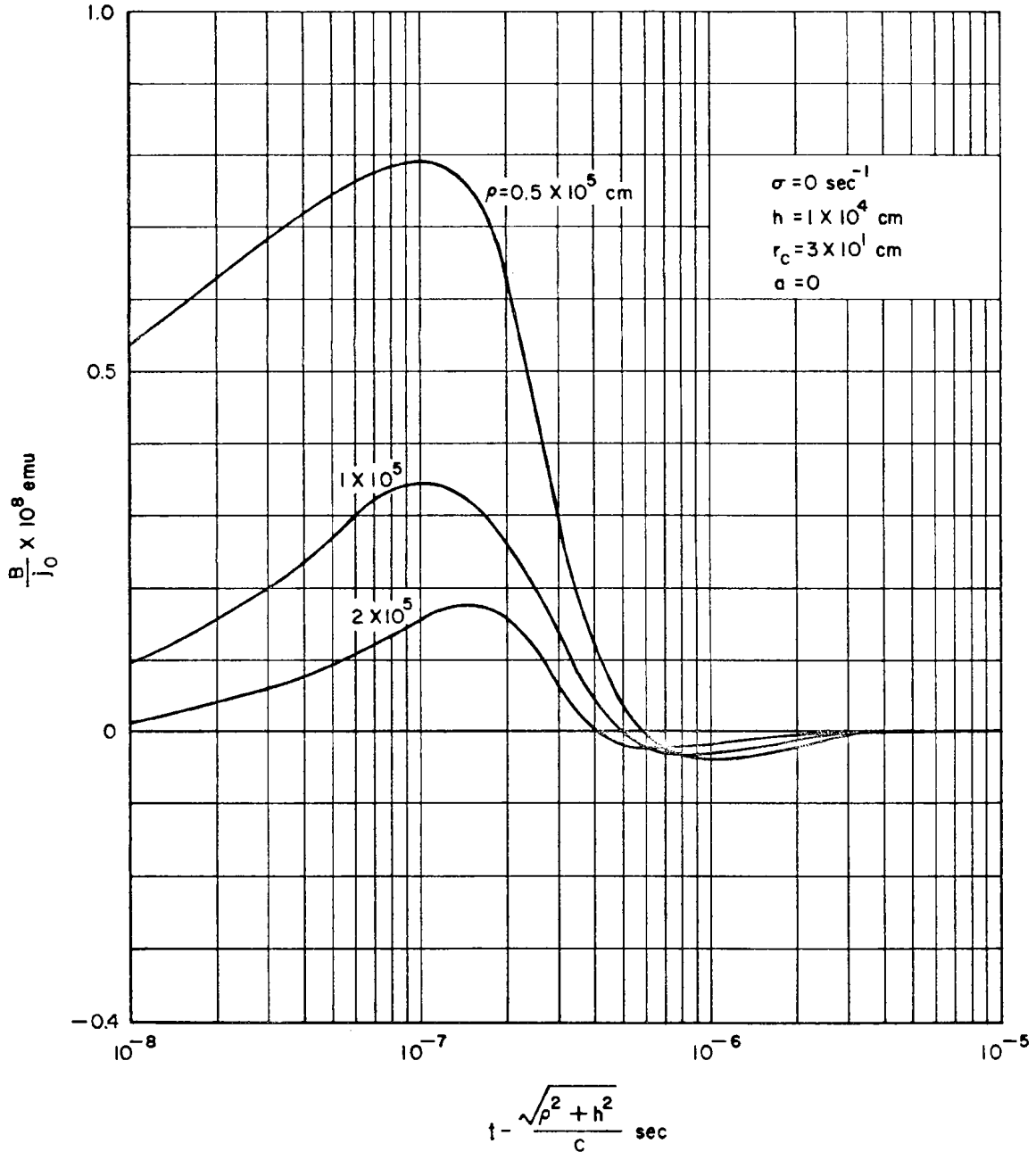
1.0
0.5
0
−0.4
$\frac{B}{j_0} \times 10^8$ emu
ρ=0.5 X 10^5 cm
1 X 10^5
2 X10^5
σ =0 sec^{-1}
h =1 X 10^4 cm
r_c=3 X 10^1 cm
a =0
10^{-8}
10^{-7}
10^{-6}
10^{-5}
$t - \frac{\sqrt{\rho^2 + h^2}}{c}$ sec

Fig. 3

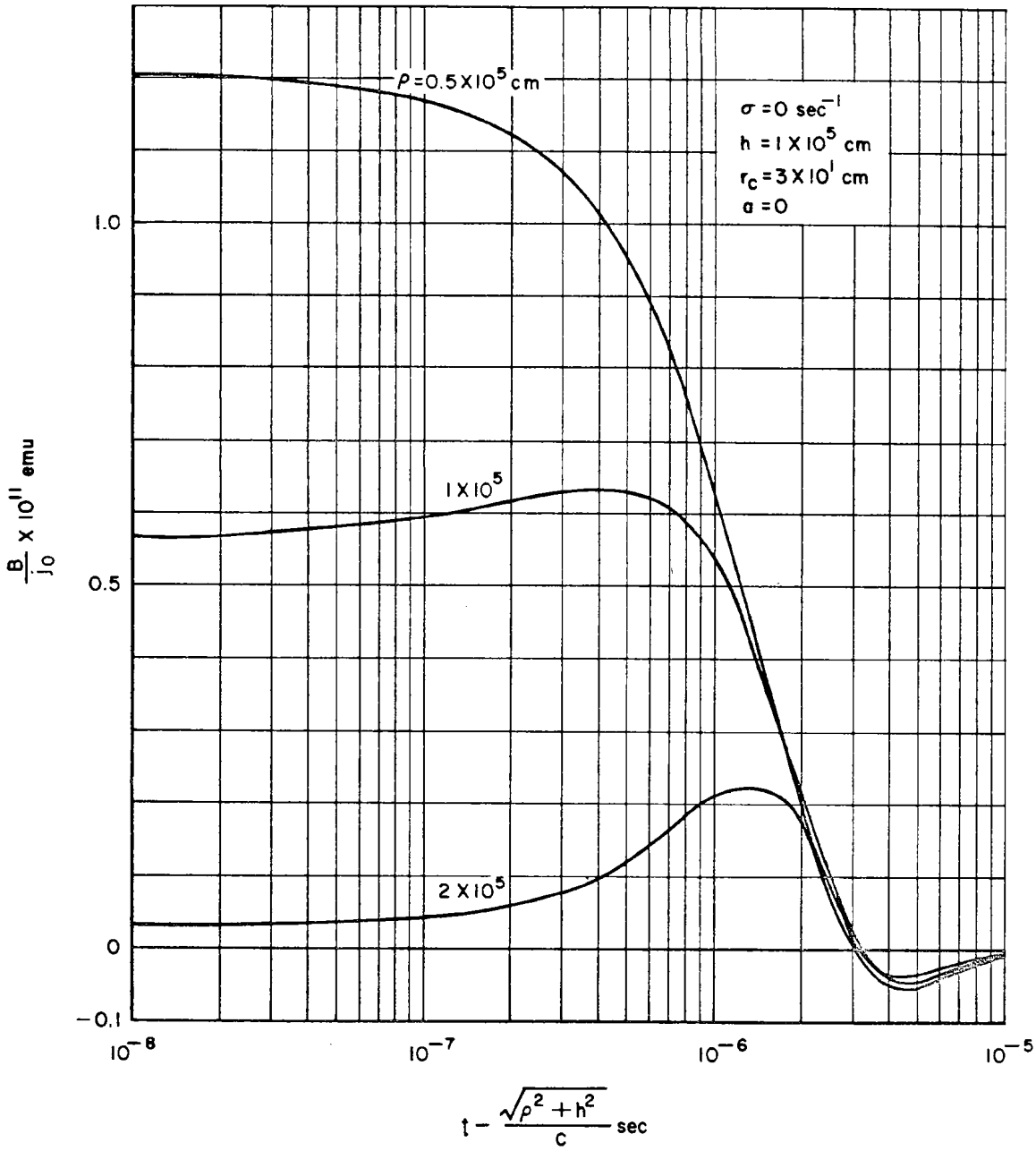
ρ=0.5X10^5 cm
σ=0 sec^-1
h=1X10^5 cm
r_c=3X10^1 cm
a=0
1X10^5
2X10^5
1.0
0.5
0
−0.1
10^-8
10^-7
10^-6
10^-5
B/j_0 X 10^11 emu
t − √(ρ^2+h^2)/c sec

Fig. 4

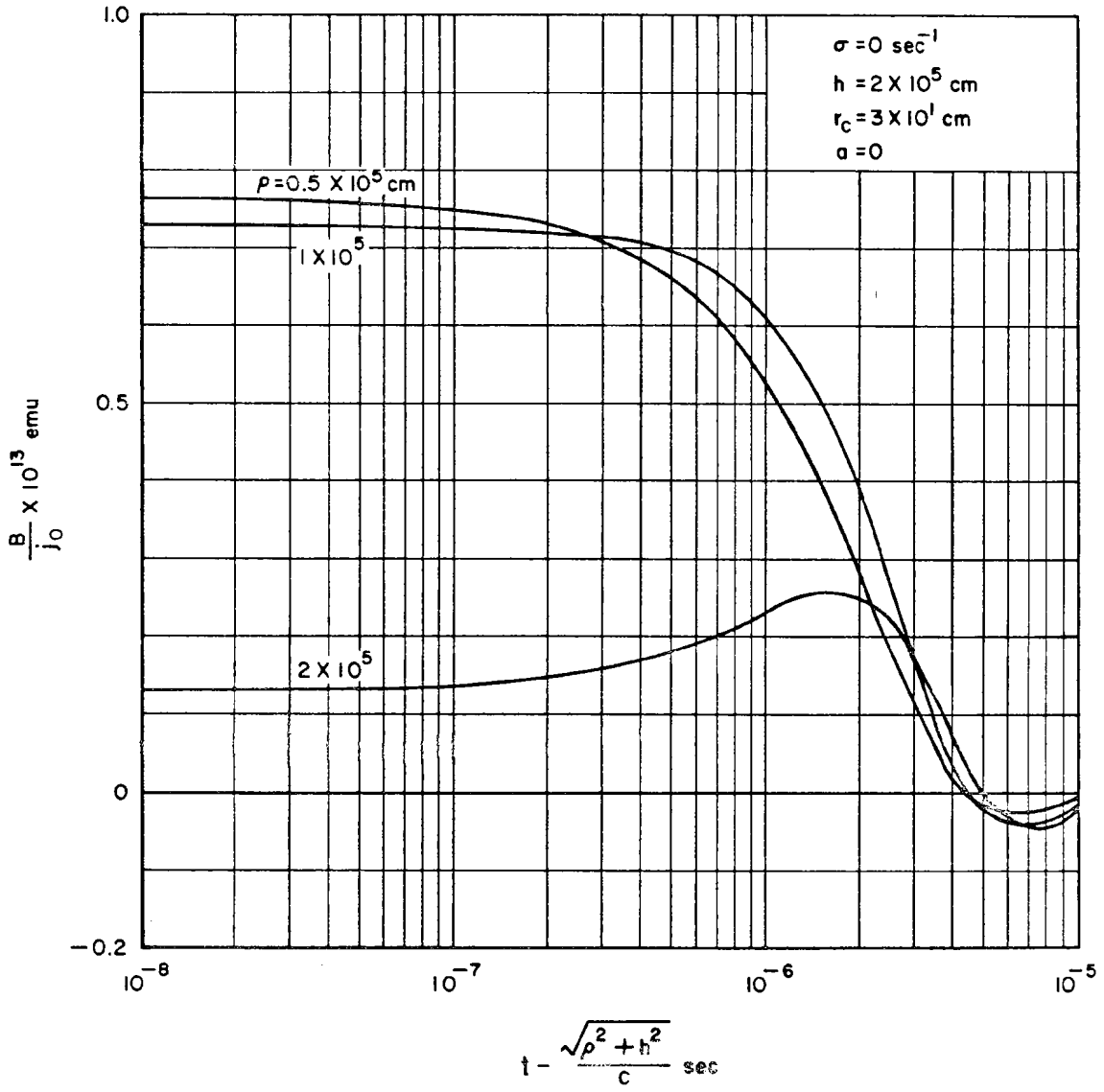
1.0
0.5
0
−0.2
$\frac{B}{j_0} \times 10^{13}$ emu
$\sigma = 0$ sec^{-1}
$h = 2 \times 10^5$ cm
$r_c = 3 \times 10^1$ cm
$a = 0$
$\rho = 0.5 \times 10^5$ cm
1×10^5
2×10^5
10^{-8}
10^{-7}
10^{-6}
10^{-5}
$t - \frac{\sqrt{\rho^2 + h^2}}{c}$ sec

Fig. 5

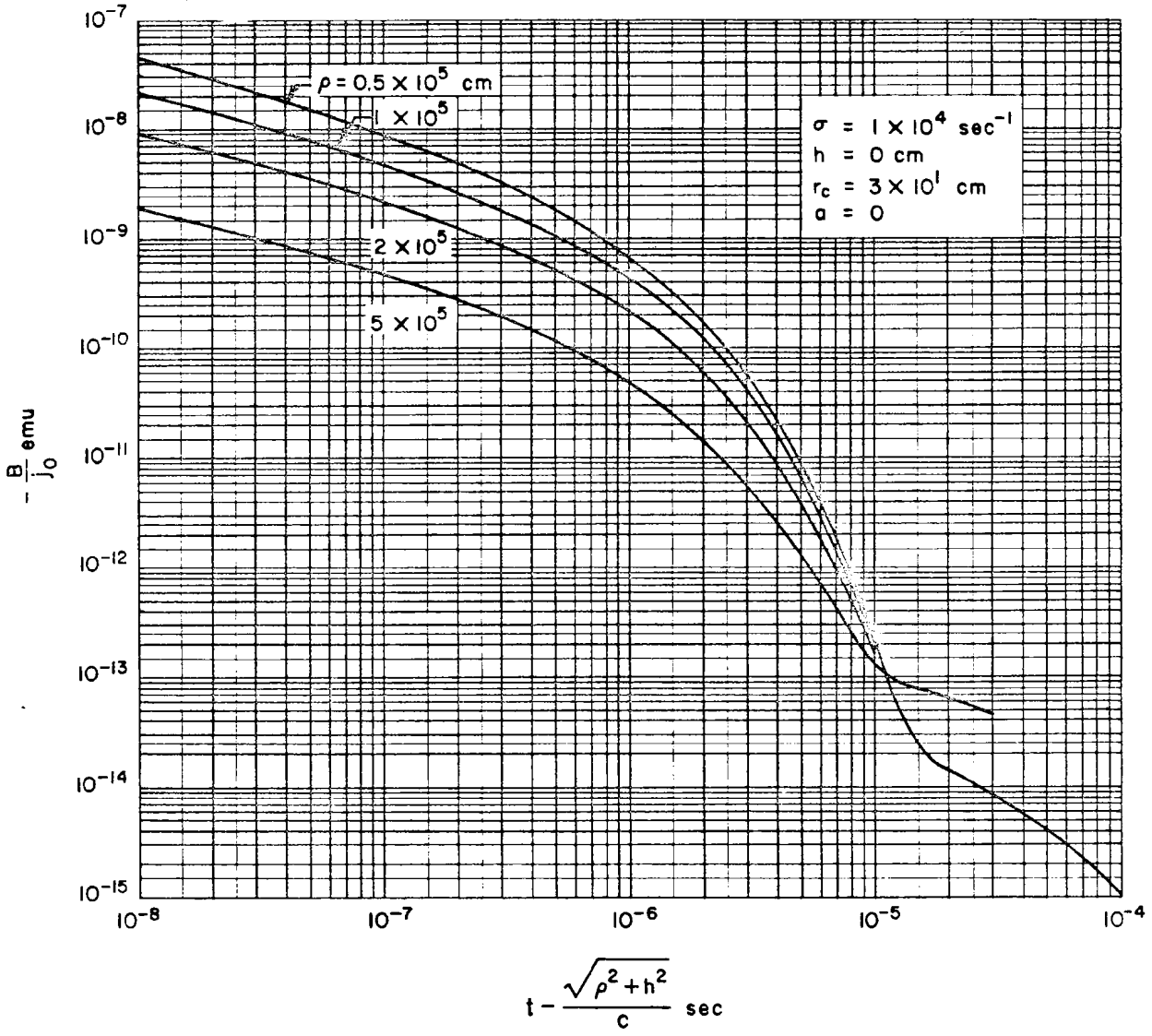
10^{-7}
10^{-8}
10^{-9}
10^{-10}
10^{-11}
10^{-12}
10^{-13}
10^{-14}
10^{-15}
$-\frac{B}{j_0}$ emu
$\rho = 0.5 \times 10^5$ cm
1×10^5
2×10^5
5×10^5
$\sigma = 1 \times 10^4$ sec^{-1}
h = 0 cm
$r_c = 3 \times 10^1$ cm
a = 0
10^{-8}
10^{-7}
10^{-6}
10^{-5}
10^{-4}
$t - \frac{\sqrt{\rho^2+h^2}}{c}$ sec

Fig. 6

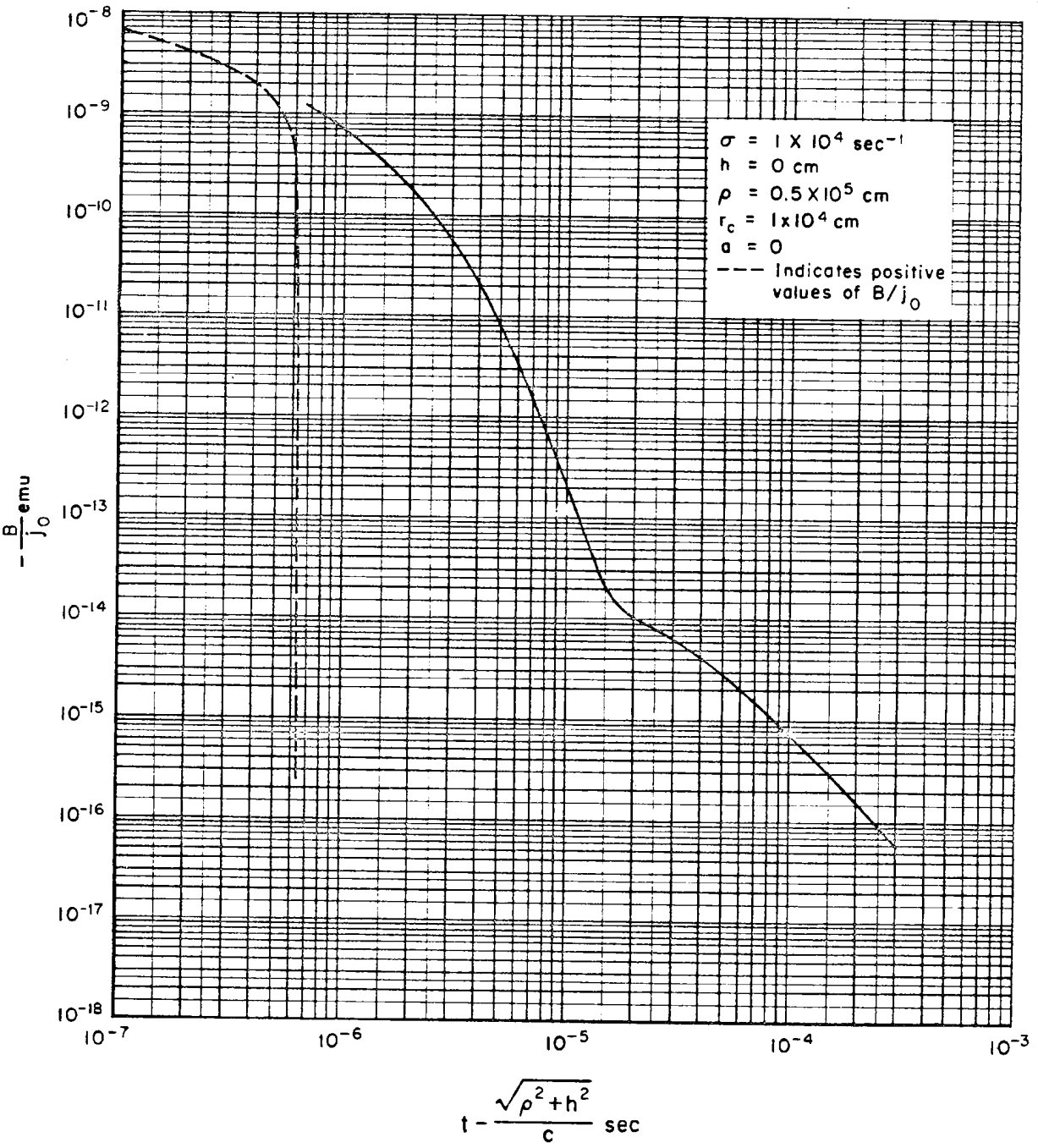
10^{-8}
10^{-9}
10^{-10}
10^{-11}
10^{-12}
10^{-13}
10^{-14}
10^{-15}
10^{-16}
10^{-17}
10^{-18}
$-\frac{B}{j_0}$ emu
10^{-7}
10^{-6}
10^{-5}
10^{-4}
10^{-3}
$t - \frac{\sqrt{\rho^2+h^2}}{c}$ sec
σ = 1 X 10^4 sec^{-1}
h = 0 cm
ρ = 0.5 X 10^5 cm
r_c = 1 x 10^4 cm
a = 0
--- Indicates positive values of B/j_0

Fig. 7

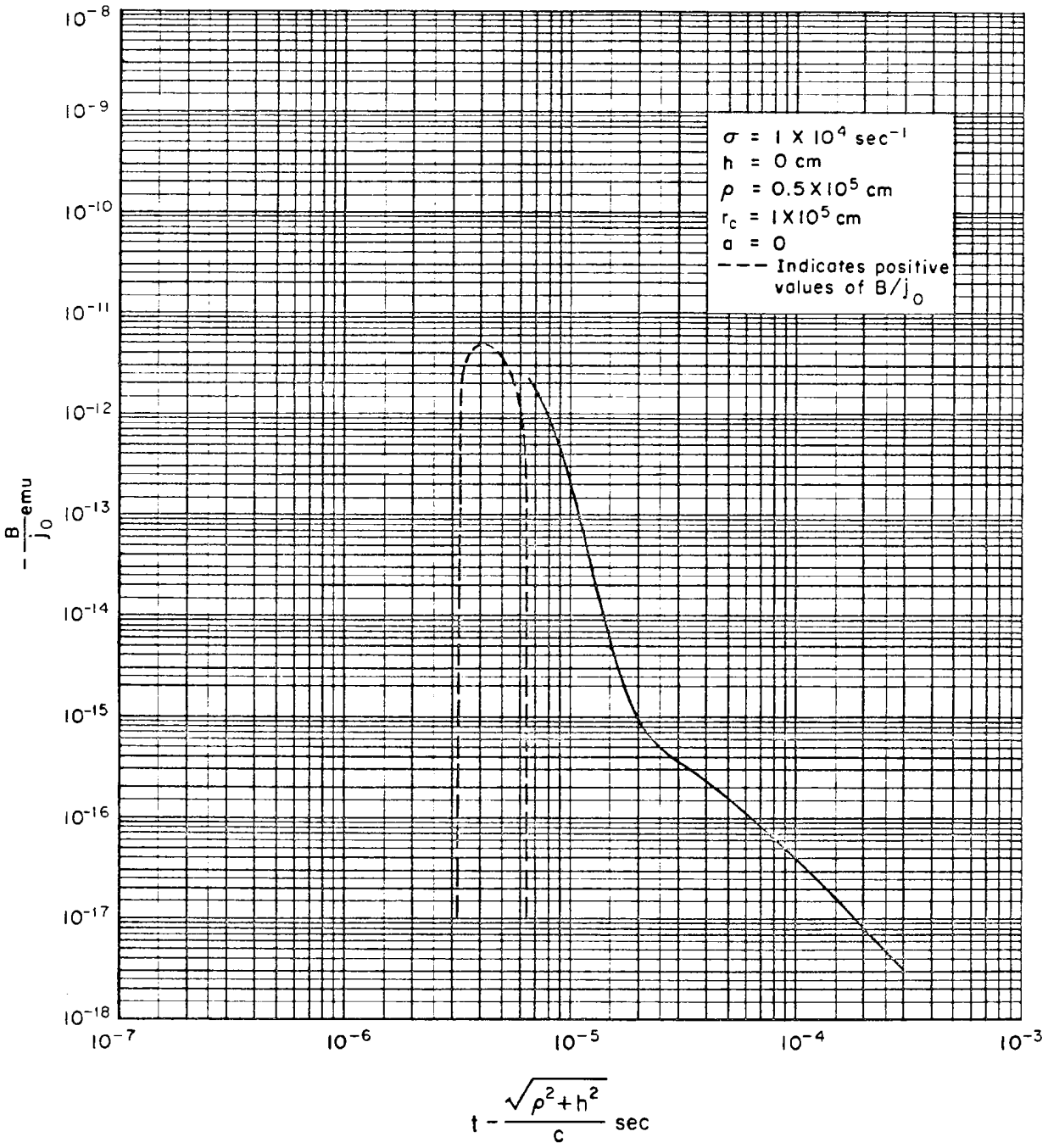
σ = 1 X 10^4 sec^{-1}
h = 0 cm
ρ = 0.5 X 10^5 cm
r_c = 1 X 10^5 cm
a = 0
--- Indicates positive values of B/j_0
$-\frac{B}{j_0}$ emu
10^{-8}
10^{-9}
10^{-10}
10^{-11}
10^{-12}
10^{-13}
10^{-14}
10^{-15}
10^{-16}
10^{-17}
10^{-18}
10^{-7}
10^{-6}
10^{-5}
10^{-4}
10^{-3}
$t - \frac{\sqrt{\rho^2+h^2}}{c}$ sec

Fig. 8

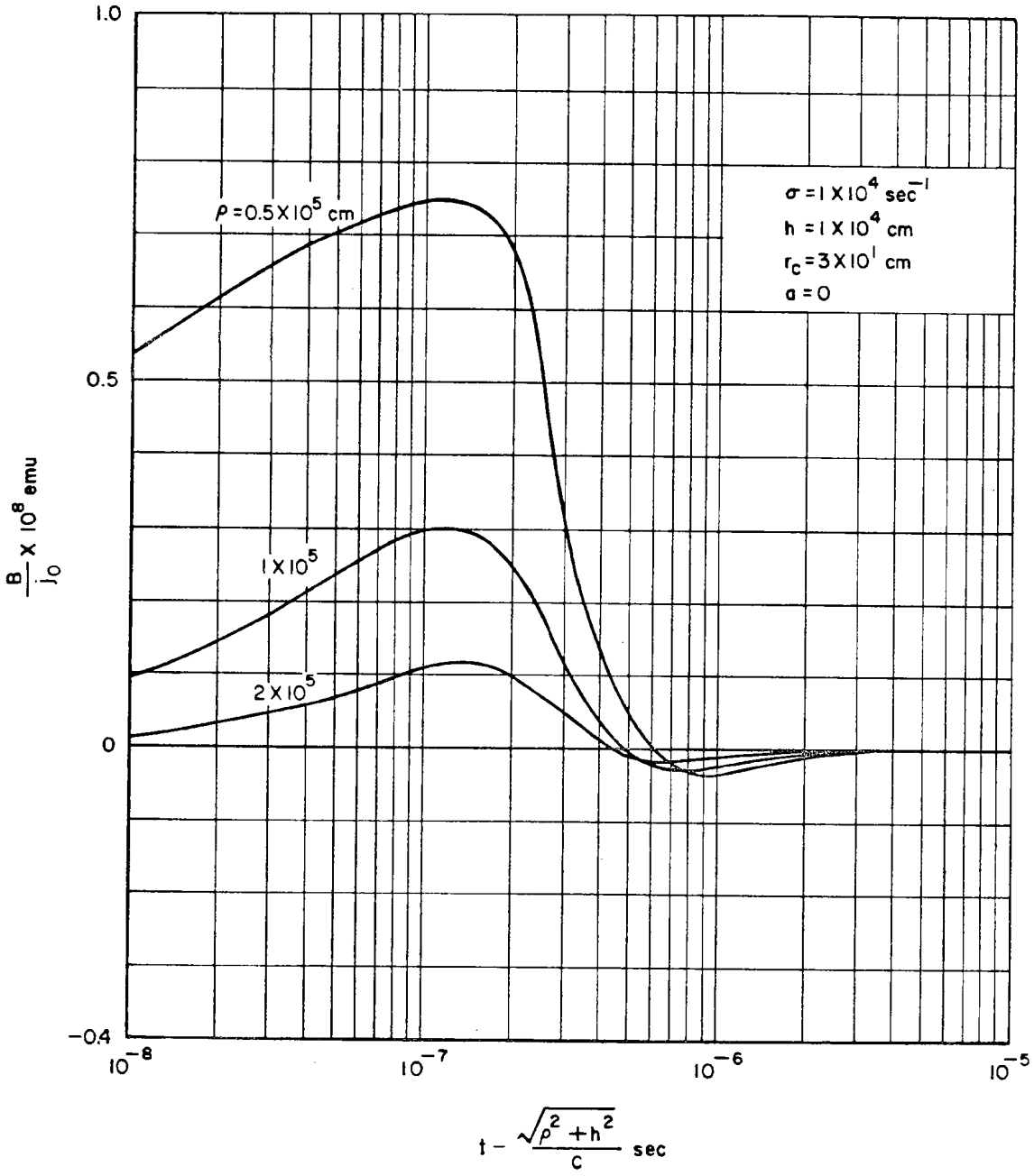
1.0
0.5
0
−0.4
$\frac{B}{j_0} \times 10^8$ emu
$\rho = 0.5 \times 10^5$ cm
1×10^5
2×10^5
$\sigma = 1 \times 10^4$ sec^{-1}
$h = 1 \times 10^4$ cm
$r_c = 3 \times 10^1$ cm
$a = 0$
10^{-8}
10^{-7}
10^{-6}
10^{-5}
$t - \frac{\sqrt{\rho^2 + h^2}}{c}$ sec

Fig. 9

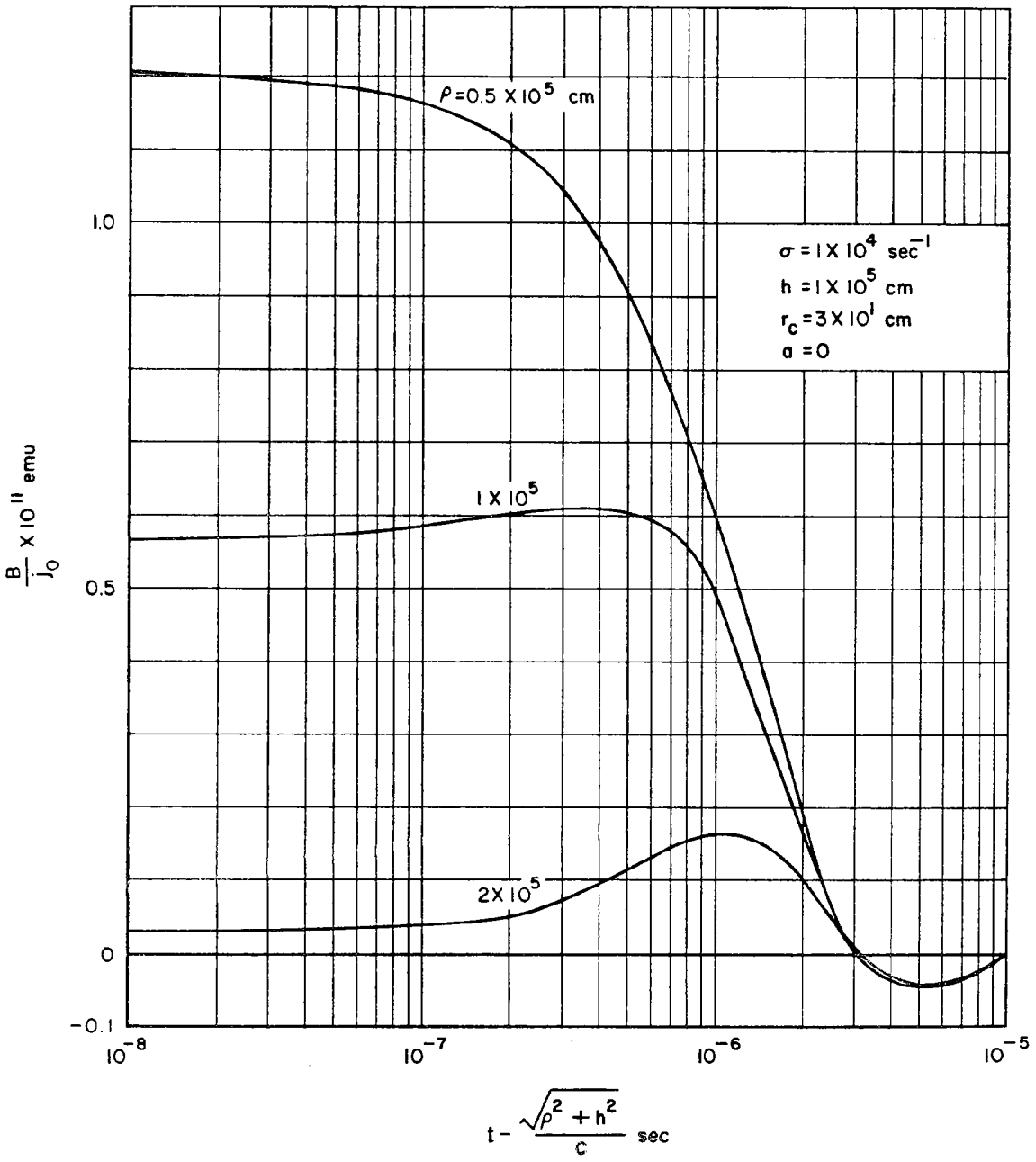
ρ=0.5 X 10^5 cm
1 X 10^5
2X 10^5
σ = 1 X 10^4 sec^-1
h = 1 X 10^5 cm
r_c = 3 X 10^1 cm
a = 0
1.0
0.5
0
-0.1
10^-8
10^-7
10^-6
10^-5
B/j_0 X 10^11 emu
t - √(ρ^2 + h^2)/c sec

Fig. 10

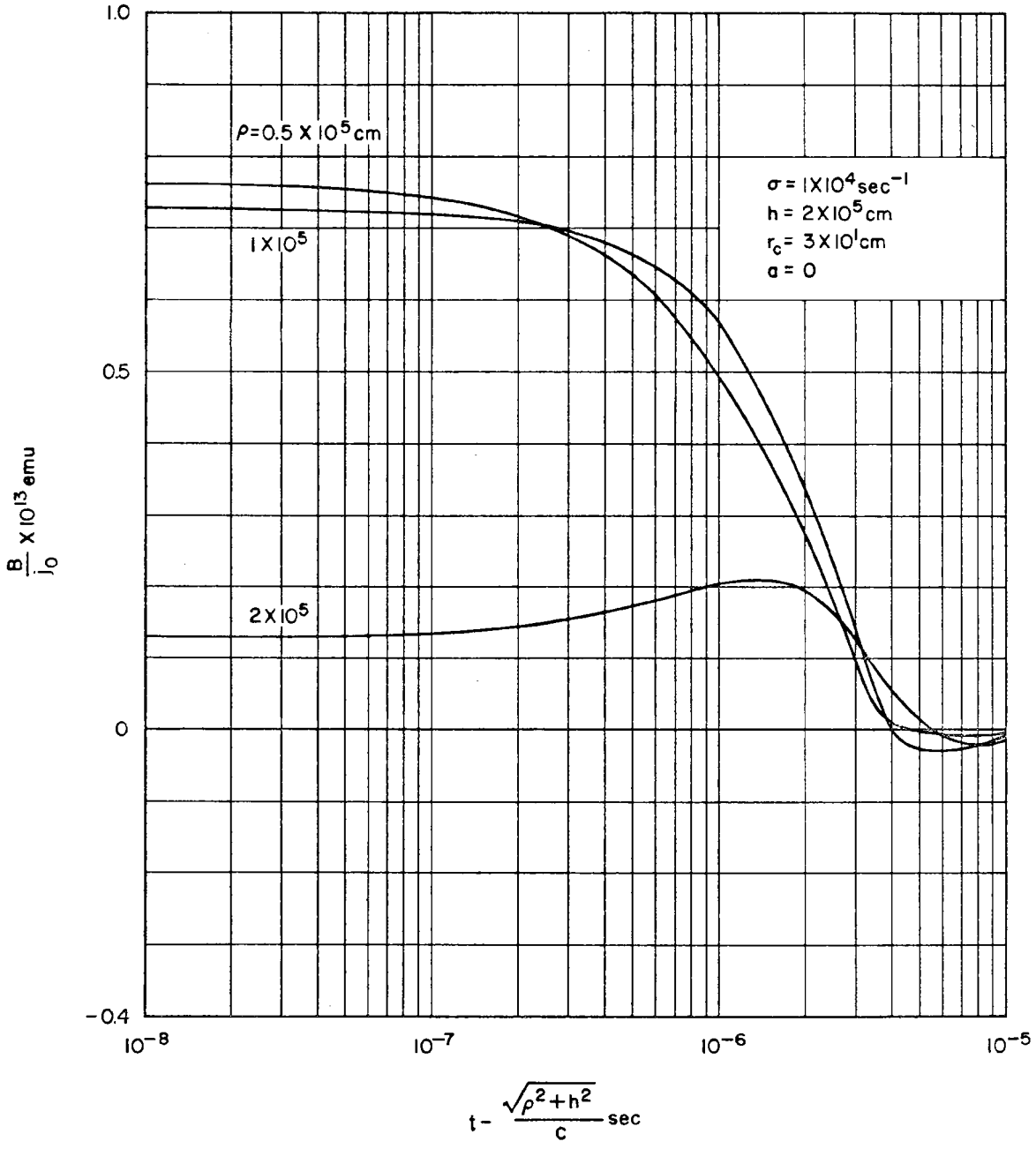
1.0
0.5
0
-0.4
ρ=0.5 X 10^{5}cm
1X10^5
2X10^5
σ = 1X10^{4}sec^{-1}
h = 2X10^{5}cm
r_c = 3X10^{1}cm
a = 0
$\frac{B}{j_0}$ X 10^{13}emu
10^{-8}
10^{-7}
10^{-6}
10^{-5}
t - $\frac{\sqrt{\rho^2+h^2}}{c}$ sec

Fig. 11

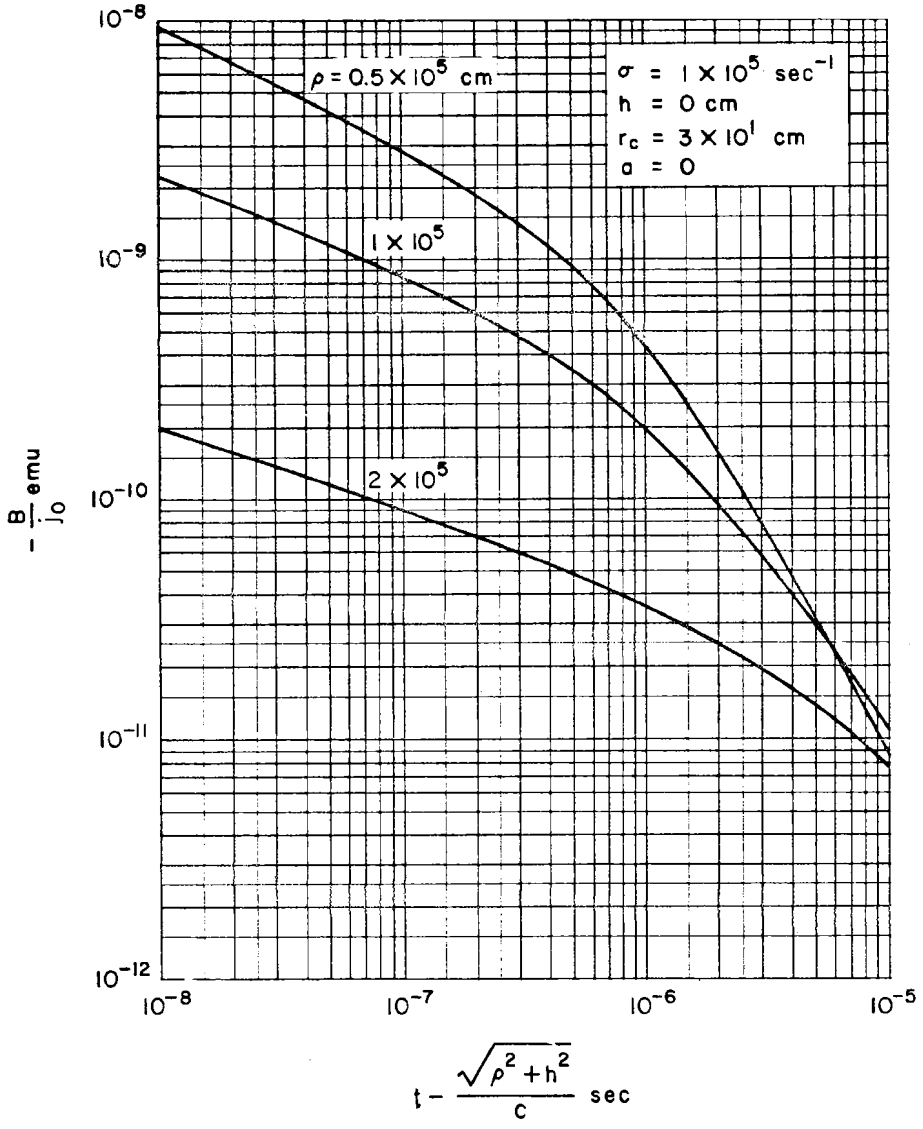
10^{-8}
10^{-9}
10^{-10}
10^{-11}
10^{-12}
$-\frac{B}{J_0}$ emu
$\rho = 0.5 \times 10^5$ cm
1×10^5
2×10^5
$\sigma = 1 \times 10^5$ sec^{-1}
h = 0 cm
$r_c = 3 \times 10^1$ cm
a = 0
10^{-8}
10^{-7}
10^{-6}
10^{-5}
$t - \frac{\sqrt{\rho^2 + h^2}}{c}$ sec

Fig. 12

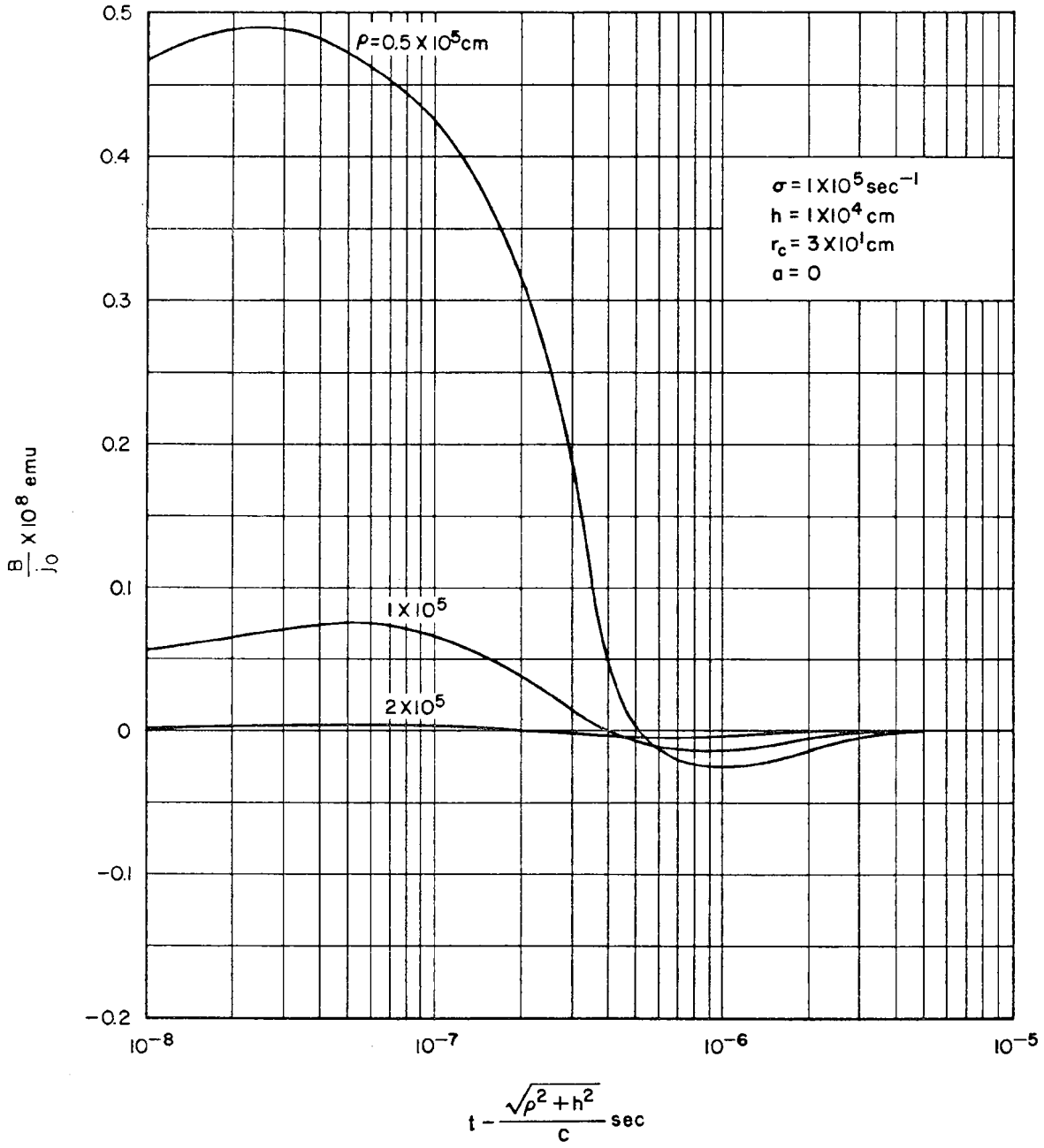
0.5
0.4
0.3
0.2
0.1
0
-0.1
-0.2
ρ=0.5 X 10^{5}cm
1X10^5
2X10^5
σ = 1X10^{5}sec^{-1}
h = 1X10^{4}cm
r_c = 3X10^{1}cm
a = 0
$\frac{B}{j_0}$ X 10^8 emu
10^{-8}
10^{-7}
10^{-6}
10^{-5}
$t - \frac{\sqrt{\rho^2+h^2}}{c}$ sec

Fig. 13

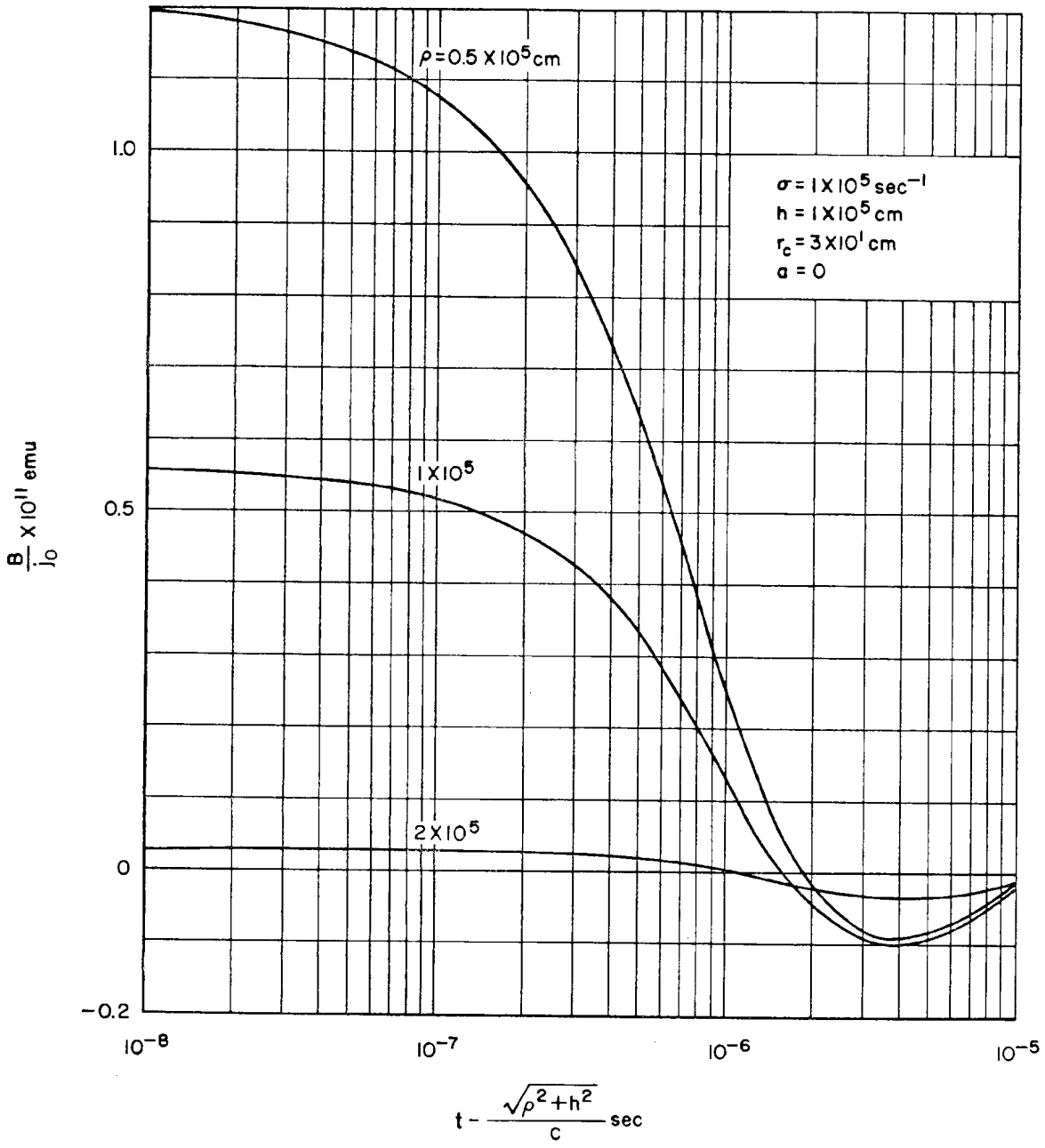
ρ=0.5 X 10^5 cm
1 X 10^5
2 X 10^5
σ = 1 X 10^5 sec^-1
h = 1 X 10^5 cm
r_c = 3 X 10^1 cm
a = 0
1.0
0.5
0
-0.2
10^-8
10^-7
10^-6
10^-5
B/I_0 X 10^11 emu
t - √(ρ^2+h^2)/c sec

Fig. 14

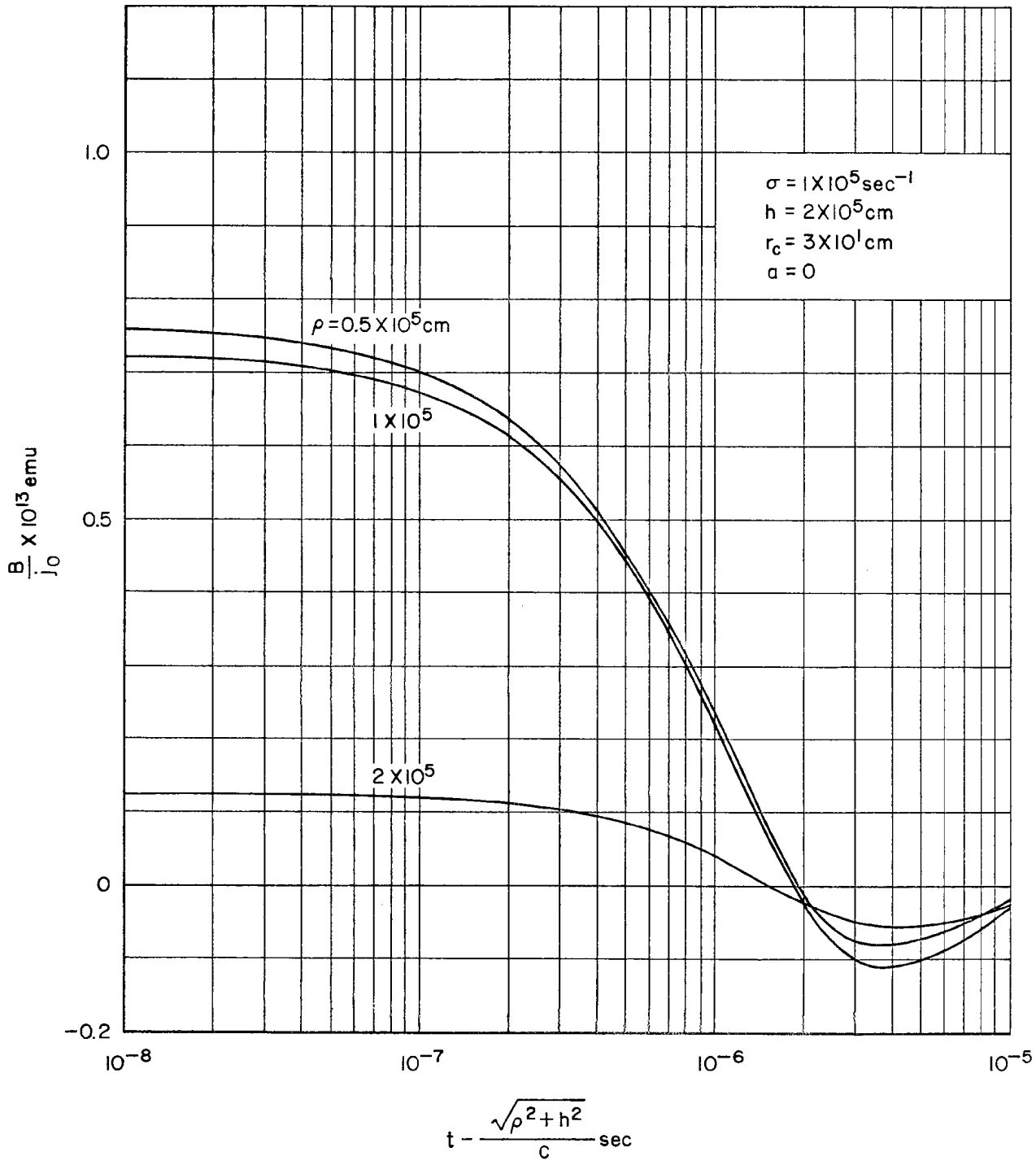
1.0
0.5
0
-0.2
$\frac{B}{J_0} \times 10^{13}$ emu
$\sigma = 1 \times 10^5 sec^{-1}$
$h = 2 \times 10^5 cm$
$r_c = 3 \times 10^1 cm$
$a = 0$
$\rho = 0.5 \times 10^5 cm$
1×10^5
2×10^5
10^{-8}
10^{-7}
10^{-6}
10^{-5}
$t - \frac{\sqrt{\rho^2 + h^2}}{c}$ sec

Fig. 15

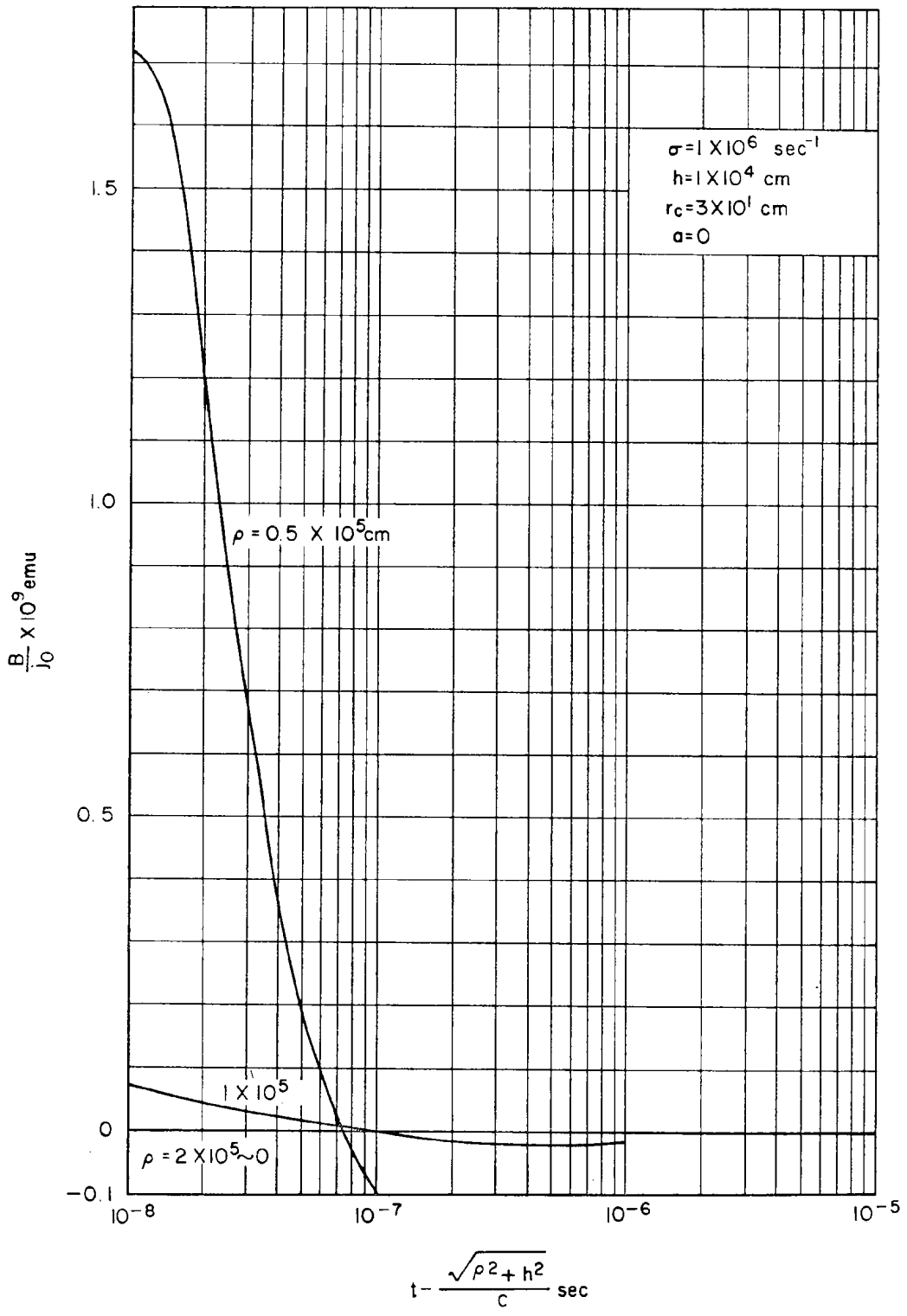
σ=1 X10^6 sec^-1
h=1 X10^4 cm
rc=3X10^1 cm
a=0
ρ = 0.5 X 10^5cm
1 X 10^5
ρ = 2 X10^5~0
1.5
1.0
0.5
0
-0.1
10^-8
10^-7
10^-6
10^-5
B/j0 X 10^9emu
t - √(ρ^2+h^2)/c sec

Fig. 16

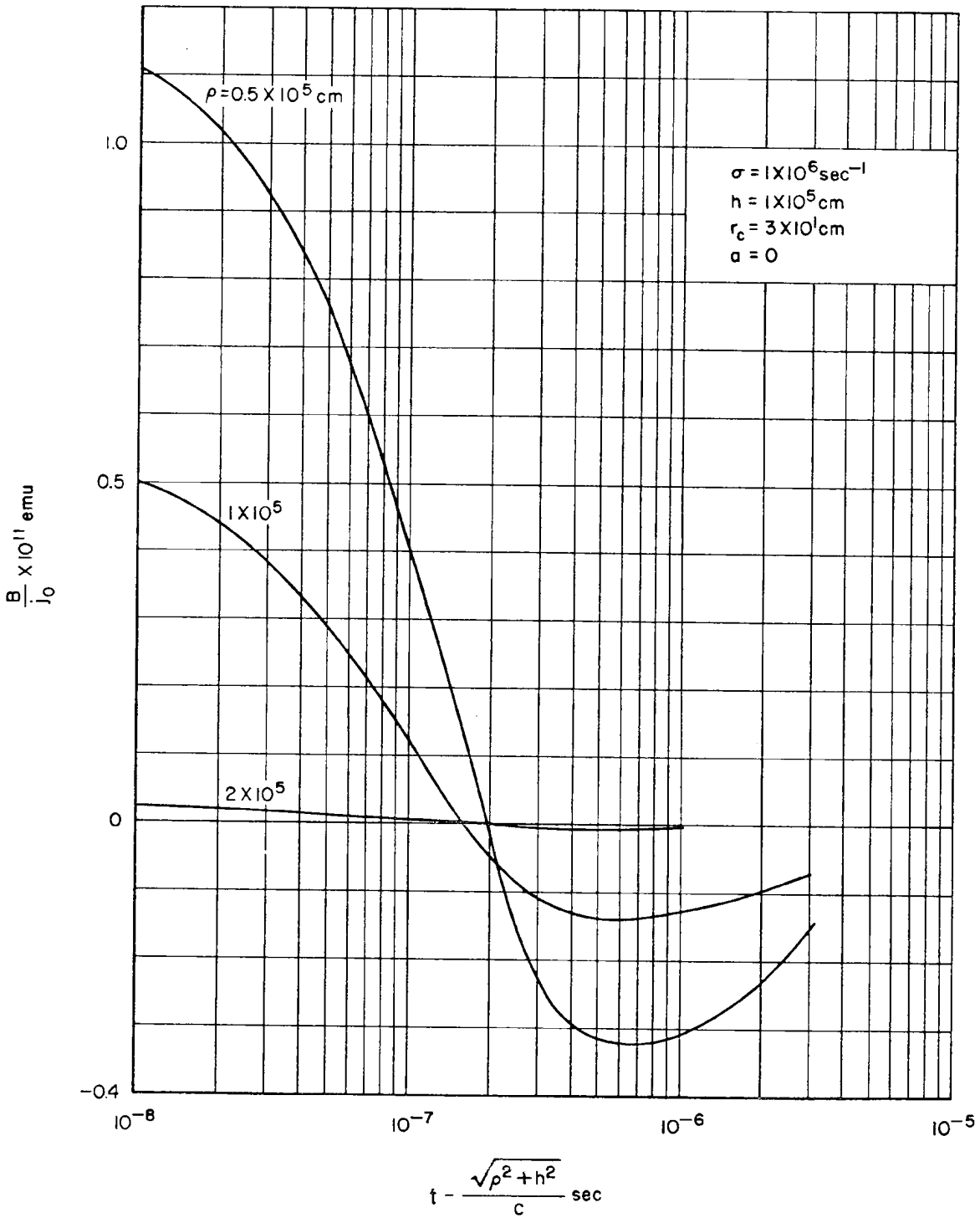
ρ=0.5X10^5 cm
1X10^5
2X10^5
σ = 1X10^6 sec^-1
h = 1X10^5 cm
r_c = 3X10^1 cm
a = 0
1.0
0.5
0
-0.4
10^-8
10^-7
10^-6
10^-5
B/J_0 X 10^11 emu
t - √(ρ^2+h^2)/c sec

Fig. 17

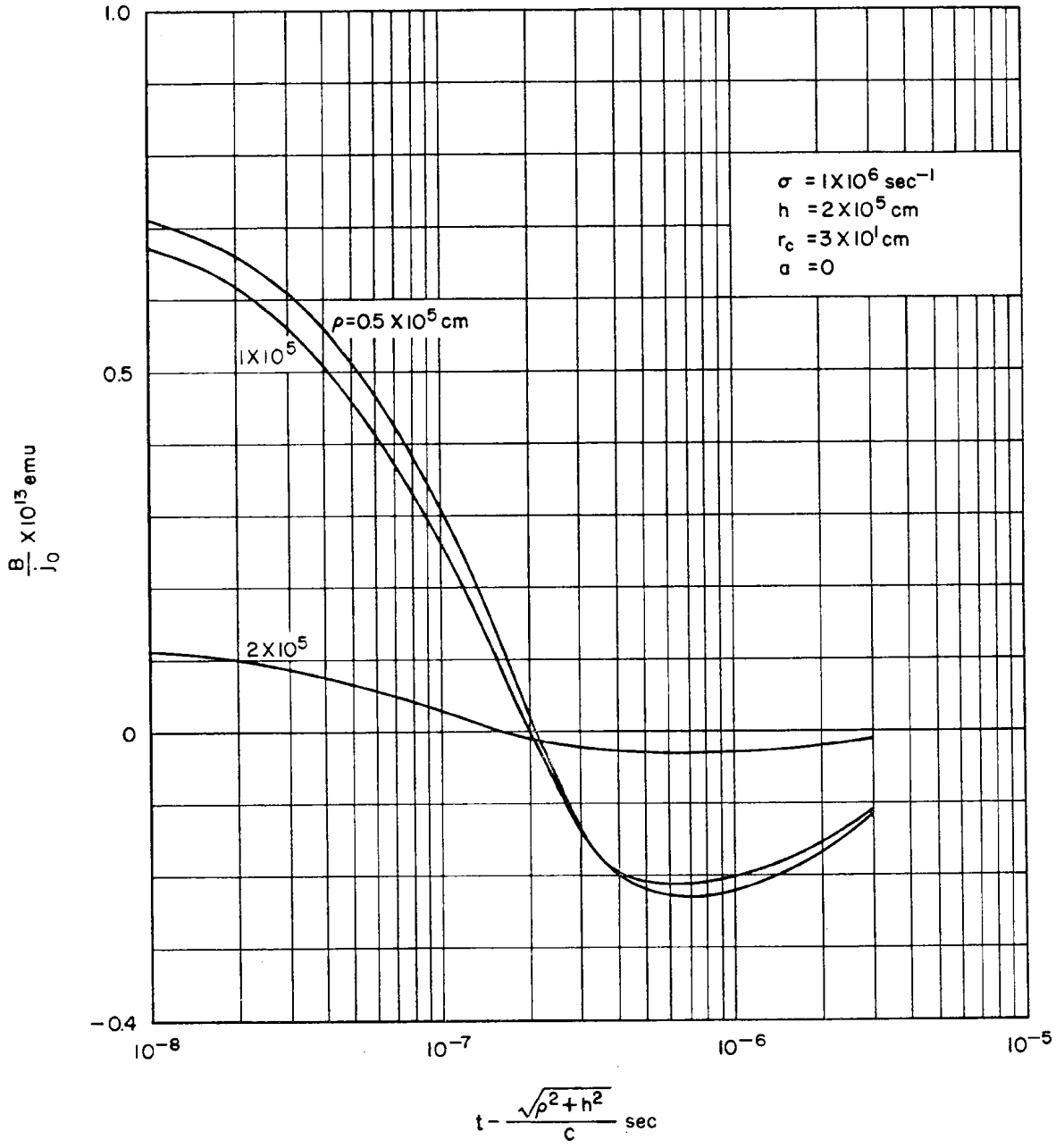
1.0
0.5
0
-0.4
10^{-8}
10^{-7}
10^{-6}
10^{-5}
$\frac{B}{J_0} \times 10^{13}$ emu
$t - \frac{\sqrt{\rho^2+h^2}}{c}$ sec
$\sigma = 1 \times 10^6$ sec^{-1}
$h = 2 \times 10^5$ cm
$r_c = 3 \times 10^1$ cm
$a = 0$
$\rho = 0.5 \times 10^5$ cm
1×10^5
2×10^5

Fig. 18